

A supernova remnant association for the fast-moving pulsar PSR J0908–4913

Simon Johnston¹* and Marcus E. Lower^{2,1}

¹*Australia Telescope National Facility, CSIRO Space and Astronomy, PO Box 76, Epping NSW 1710, Australia*

²*Centre for Astrophysics and Supercomputing, Swinburne University of Technology, PO Box 218, Hawthorn, VIC 3122, Australia*

Last updated; in original form

ABSTRACT

A recent measurement of the proper motion of PSR J0908–4913 shows that it is a fast moving object at a distance of some 3 kpc. Here we present evidence that the pulsar is located at the edge of a previously unknown, filled-centre supernova remnant, G270.4–1.0. The velocity vector of the pulsar points directly away from the centre of the remnant. The putative association of the pulsar with SNR G270.4–1.0 implies the pulsar is ~ 12 kyr old, significantly less than its characteristic age of 110 kyr. We show that the rotation axis of the pulsar points in the direction of the proper motion. Rotation measure and dispersion measure variations are seen over time, likely indicating the pulsar is passing behind a filament of the remnant.

Key words: pulsars:general – pulsars: individual: PSR J0908–4913

1 INTRODUCTION

PSR J0908–4913 was first discovered by D’Amico et al. (1988). It has a spin period of 106 ms and a dispersion measure (DM) of $180.4 \text{ cm}^{-3} \text{ pc}$. The spin-down energy of the pulsar is high ($4.9 \times 10^{35} \text{ ergs}^{-1}$) and its characteristic age is 110 kyr. As pulsars go, this particular object has a lot to offer. First, it is one of the few pulsars for which we see radio emission from both magnetic poles (as originally identified by D’Amico et al. 1988). This means that the geometry of the pulsar is well determined (Kramer & Johnston 2008; Johnston & Kramer 2019), another rarity in the pulsar population. It emits gamma-rays (Abdo et al. 2013), as expected for highly-energetic pulsars which are orthogonal rotators (Johnston et al. 2020b), and has been weakly detected at X-ray wavelengths (Kargaltsev et al. 2012). The pulsar powers a pulsar wind nebula and its motion through the interstellar medium produces a radio bow-shock (Gaensler et al. 1998). Finally, large DM variations are seen (Petroff et al. 2013), making the pulsar an excellent probe of the interstellar medium. Most recently, measurements of its proper motion imply it is a fast-moving object Lower et al. (2021), contrary to previous results (Johnston et al. 1998).

In this paper we explore the implications of the newly measured proper motion, describe a putative supernova remnant association and present the dispersion measure and rotation measure history of the pulsar over 15 years’ worth of observations.

2 DISTANCE

The distance to PSR J0908–4913 has not been directly determined through parallax measurements. We are therefore reliant on distance

estimates based either on the pulsar’s dispersion measure or spectroscopy and, for this pulsar, these distance estimates have a chequered history. In the discovery paper, D’Amico et al. (1988) estimated a distance of 3 kpc based on the DM. The next iteration of distance models increased this estimate to 6.6 kpc (Taylor & Cordes 1993). H_I measurements in the direction of the pulsar by Koribalski et al. (1995) showed clear absorption features which enabled them to place a lower distance limit of 2.4 kpc and an upper distance limit of 6.7 kpc to the pulsar. Cordes & Lazio (2002) incorporated the H_I limits into their model and their estimate to the distance of the pulsar was only 2.6 kpc. Finally, in the latest published model of the Galactic electron density, Yao et al. (2017) have a distance estimate of a mere 1.0 kpc, clearly not compatible with the H_I lower limit.

One final piece of information is the detection of pulsed gamma-ray emission from the pulsar (Abdo et al. 2013). At a distance of 1.0 kpc, the efficiency of the pulsar in gamma-rays is only 0.6%, at the low end of the scale for pulsars of this type (Abdo et al. 2013). A distance of 2.5 to 3.0 kpc raises the efficiency to 4–5%, more in line with expectations. In X-rays this works in the opposite direction. Kargaltsev et al. (2012) report an X-ray efficiency of 5.7×10^{-5} at a distance of 6.6 kpc, and this decreases to only 1.2×10^{-5} with the closer distance estimate. We return to the distance problem in the next section.

3 SPACE VELOCITY

A comprehensive study of the scintillation of southern pulsars, including PSR J0908–4913, was carried out by Johnston et al. (1998). From a single 3 h observation of the pulsar at 1520 MHz, they derived a scintillation bandwidth of 12 MHz and a very long scintillation timescale of 4770 s. This implies a scintillation velocity of only $\sim 50 \text{ kms}^{-1}$ at their adopted distance of 6.7 kpc (and hence an even lower value if the distance is 3 kpc).

* E-mail: simon.johnston@csiro.au

It became apparent that the scintillation bandwidth as derived by Johnston et al. (1998) was in error. In particular, evidence for a scatter-broadened profile at lower frequencies indicates a much smaller value for the scintillation bandwidth than they derived. In the geometric modelling by Kramer & Johnston (2008), they estimated a scintillation bandwidth of only 2500 Hz at 1.4 GHz. Additionally, there are no obvious scintillation bands present in recent data taken with the Parkes telescope at frequencies between 700 and 4000 MHz (Johnston et al. 2021), while data taken at 8.5 GHz (Johnston et al. 2006) showed narrow scintillation structures. To clear up the scintillation question, we collected data using the Parkes radio telescope at an observing frequency of 8.5 GHz on 2021 Feb 26. The total bandwidth was 1024 MHz subdivided into 1024 channels each of width 1 MHz, with a total integration time of 6930 s subdivided into 30 s blocks. Polarization calibration was performed via observations of a pulsed square-wave injected directly into the feed. Flux calibration was carried out using observations of PKS B1934–638 which has a flux density of 2.8 Jy at 8.5 GHz. The flux density of the pulsar was computed for each time-step in each frequency channel to create a dynamic spectrum. These data were then analysed using `SCINTOOLS`¹ as described in Reardon et al. (2020). The decorrelation bandwidth, $\Delta\nu_d$, was computed to be 3.2 MHz and the scintillation time, t_d , to be 59 s. As a check of these numbers, we obtained the 2005 data at 8.356 GHz from the Parkes pulsar data archive² and applied the same software tools. This yielded 2.8 MHz and 56 s for the scintillation bandwidth and time, both in good agreement with the more recent data. The scintillation velocity, V_{ISS} is given by

$$V_{ISS} = A_V \frac{(D\Delta\nu_d)^{1/2}}{\nu t_d}, \quad (1)$$

where D is the distance to the pulsar in kpc, ν is the observing frequency in GHz, $\Delta\nu_d$ is in MHz and t_d is in s. The constant A_V is derived by assuming a Kolmogorov turbulence spectrum and a homogeneously turbulent medium, and has been estimated as 3.85×10^4 . For $D = 3$ kpc, using the values determined above yields $V_{ISS} = 250 \text{ km s}^{-1}$.

Modern inference techniques have been brought to bear on the timing of the pulsar over two decades. This enabled Lower et al. (2021) to determine a proper motion of $-37 \pm 9 \text{ mas yr}^{-1}$ in right ascension and $31 \pm 10 \text{ mas yr}^{-1}$ in declination. This leads to an overall proper motion of $47 \pm 9 \text{ mas yr}^{-1}$, hence a transverse velocity of $670 \pm 130 \text{ km s}^{-1}$ assuming a distance of 3 kpc at an angle of $50^\circ \pm 11^\circ$ measured from north towards west. We note that the velocity is already high compared to the bulk of the pulsar population (e.g. Hobbs et al. 2005) and it therefore seems unlikely that the pulsar can be as distant as 7 kpc. In Galactic coordinates, the pulsar’s velocity is oriented almost entirely in the negative longitude direction with only a small component in the latitude direction. With the pulsar now more than 1° (60 pc at a distance of 3 kpc) from the Galactic plane, it seems as if it did not originate from zero latitude. It should be noted that the bulk of the emission from the Galactic plane at these longitudes is at negative latitudes.

There remains a significant discrepancy between the scintillation velocity and the proper motion. One way to reconcile the two values would be to postulate that the scattering screen lies significantly closer to the pulsar than to the observer.

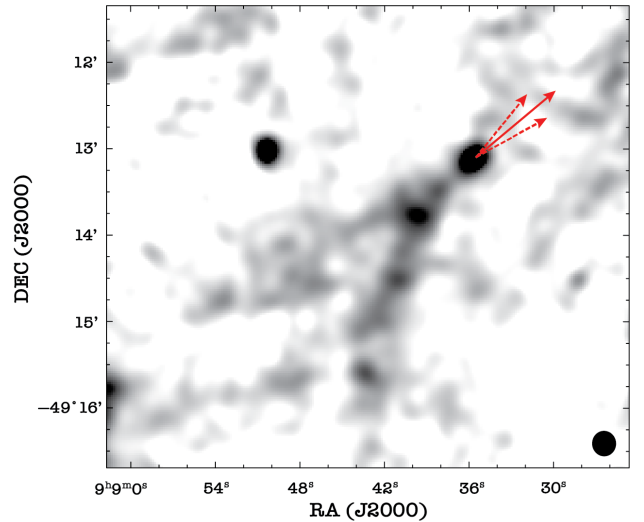


Figure 1. Radio image at 1.3 GHz from observations in 1997 with the Australia Telescope Compact Array, adapted from Gaensler et al. (1998). The synthesised beam ($17.7'' \times 16.6''$ at position angle 5°) is shown in the bottom right. Proper-motion direction from Lower et al. (2021) is shown by the solid-red arrow. Uncertainty in the proper motion is represented by the dashed red arrows.

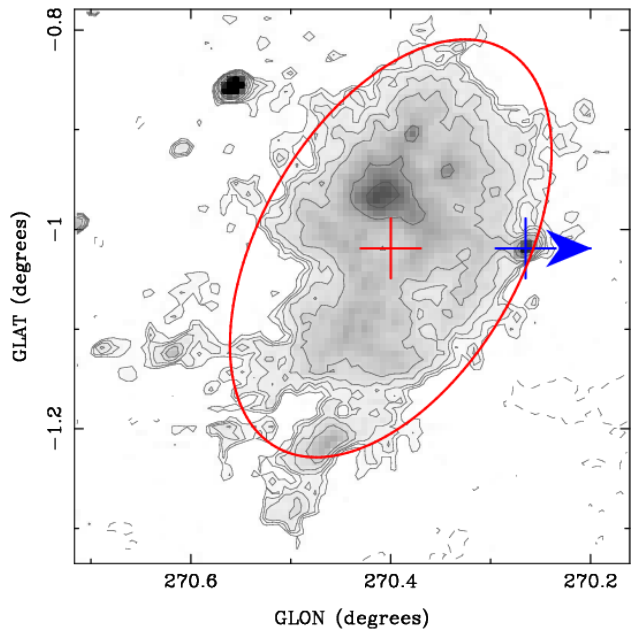


Figure 2. Radio image at 843 MHz in Galactic coordinates taken from the Molonglo Galactic Plane Survey of the region surrounding PSR J0908–4913. Observations were taken in 1991, the synthesised beam measures $43'' \times 57''$. The blue cross denotes the location of the pulsar with the arrow showing the direction of the proper motion. The red ellipse marks the approximate region of the SNR, with the centre of the ellipse shown by the red cross.

4 WIND NEBULA

More than twenty years ago, a search for pulsar wind nebulae (PWN) around southern (Stappers et al. 1999) and northern pulsars (Frail & Scharringhausen 1997) was carried out. Although some 60 sources were surveyed, only one clear example of a pulsar harbouring a PWN,

¹ <https://github.com/danielreardon/scintools>

² <https://data.csiro.au/dap/>

PSR J0908–4913 (Gaensler et al. 1998), was found. In addition to the PWN surrounding the pulsar, a clear trail or bow-shock was seen in the radio image which is reproduced in Figure 1. The pulsar is one of only a small handful of pulsars known to have radio PWN. The Gaensler et al. (1998) interpretation of these structures was based on a distance estimate of 7 kpc and a low velocity of 60 km s^{-1} . This led to the conclusion that the pulsar was moving through a very dense medium (hydrogen density n_{H} of 2 cm^{-3}) and that the bow-shock emission was the same age as the pulsar ($\sim 10^5 \text{ yr}$). Figure 1 also shows the proper motion vector as determined by Lower et al. (2021), pointing in exactly the direction predicted by Gaensler et al. (1998).

Our understanding now is that the pulsar is moving some ten times faster than they assumed and that the distance is less than half the previous value. This leads to a very different interpretation. The PWN is unresolved at this resolution, so we assume the stand-off distance, r_s must be $< 1.2 \times 10^{15} d \text{ cm}$ (with d in kpc). If we assume that the entire spin-down energy of the pulsar goes into the PWN and we equate this with the ram pressure due to the pulsar’s velocity, then we can compute the hydrogen density must be $n_{\text{H}} \sim 0.08 \text{ cm}^{-3}$. This value can be higher if r_s is smaller than assumed but can also be lower if the efficiency of the pulsar in producing a particle wind is not 100%. With those caveats, we no longer need the extreme value of n_{H} derived by Gaensler et al. (1998) and our value is more in line with that expected from the interstellar medium in general (e.g. McKee & Ostriker 1977). Furthermore, we see that the bow-shock length of 3 arcmin equates to some 2.5 pc assuming a distance of 3 kpc. With a pulsar velocity of 670 km s^{-1} , the duration of the emission from the bow-shock must be less than 10^4 yr before it fades into the medium. Two explanations for this are possible. First, the observations may not be sensitive enough to show the low surface-brightness structures far from the pulsar. Secondly, we do not have a good handle on the spectrum of the PWN in order to determine a break frequency from the ageing of the synchrotron electrons. This could in turn allow us to determine the magnetic field within the PWN: a high value (above 1 mG) would strongly limit the lifetime. We note that any X-ray nebula must be faint as Kargaltsev et al. (2012) report only 10 photons from a 35 ks *Chandra* observation of the region around the pulsar.

However, it appears to be the case that the structure seen in the high resolution image is only part of a much larger, low surface brightness structure. A radio image from the Molonglo Galactic Plane Survey (Green et al. 1999; Murphy et al. 2007) at the pulsar’s location is shown in Figure 2. Could this be a filled-centre supernova remnant (SNR) created by the same supernova that formed the pulsar? The pulsar is currently situated on the edge of the structure with its proper motion vector points directly away from the centre of emission, lending credence to a link between the two. We also note the similarities between this and several other systems: SNR W44 with PSR B1853+01 (Jones et al. 1993; Frail et al. 1996), CTB 80 with PSR B1951+32 (Castelletti et al. 2003), PSR J0002+6216 with CTB 1 (Schinzel et al. 2019), PSR J0538+2817 with S147 (Kramer et al. 2003; Ng et al. 2007) and SNR G5.4–1.2 with PSR B1757–24 (Manchester et al. 1991; Gaensler & Frail 2000). In W44, CTB 80 and S147 the pulsar is embedded within the shell, whereas in G5.4–1.2, the pulsar has just exited its parent shell and in CTB 1 the high-velocity pulsar has escaped its shell entirely. In all five of these systems, an elongated PWN along the direction of motion is seen.

We therefore assume that the structure seen in Figure 2 is indeed a supernova remnant, to which we assign the name SNR G320.4–1.0. The SNR is roughly ellipsoidal, and an estimate of its centre is shown by the red cross in Figure 2. If the pulsar was born in

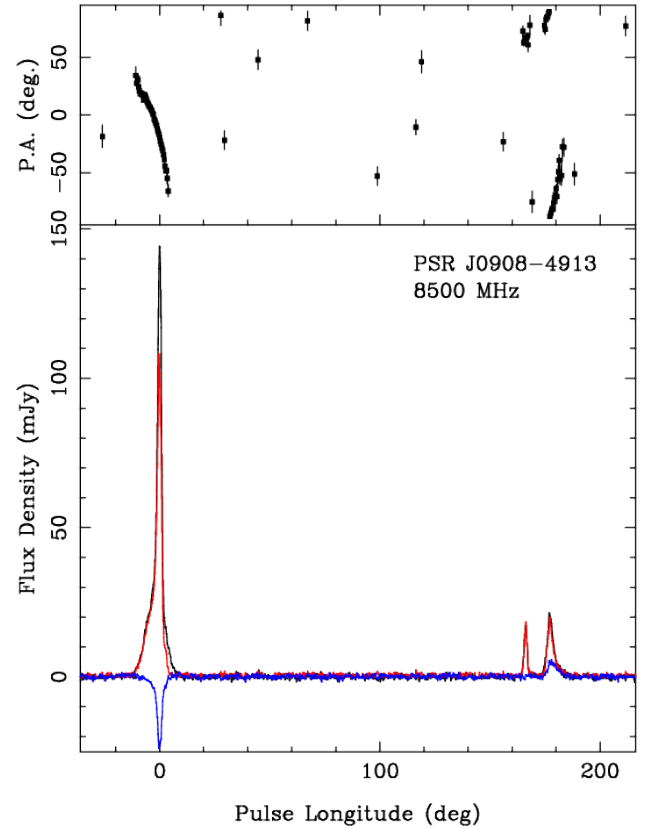


Figure 3. Flux and polarization calibrated profile of PSR J0908–4913 at 8.5 GHz. The bottom panel shows total intensity (black), linear polarization (red) and circular polarization (blue). The top panel shows the position angle of the linear polarization at infinite frequency.

the same explosion as created the SNR, its current displacement of some 10 arcmin from the centre of the SNR and its proper motion of $\sim 47 \text{ mas yr}^{-1}$ yield a kinematic age of $\sim 12.7 \text{ kyr}$ (a value which is independent of the distance). The characteristic age, τ_c , of the pulsar given by $\tau_c = P/(2\dot{P})$ where P is the spin period and \dot{P} its derivative is 110 kyr, considerably higher than the kinematic age. In the examples of similar systems mentioned above, that the kinematic age of PSR B1757–24 is much larger than its τ_c (Gaensler & Frail 2000), with the opposite being true for PSR B1951+32 (Zeiger et al. 2008), PSR J0002+6216 (Schinzel et al. 2019) and PSR J0538+2817 (Kramer et al. 2003), while for PSR B1853+01 the ages roughly agree. It should be noted that τ_c comes with several caveats; it assumes a very fast initial spin period and a braking index of $n = 3$, neither of which are well established (Johnston & Karastergiou 2017; Parthasarathy et al. 2020). To reconcile τ_c with the kinematic age in PSR J0908–4913 then either it was born spinning with a period not too different from its current spin period and has $n = 3$, or it was born spinning fast and has n of order 20 (Johnston & Karastergiou 2017). Curiously and perhaps coincidentally, a value of $n = 23$ has been determined by Lower et al. (2021) following nearly three decades of timing this pulsar.

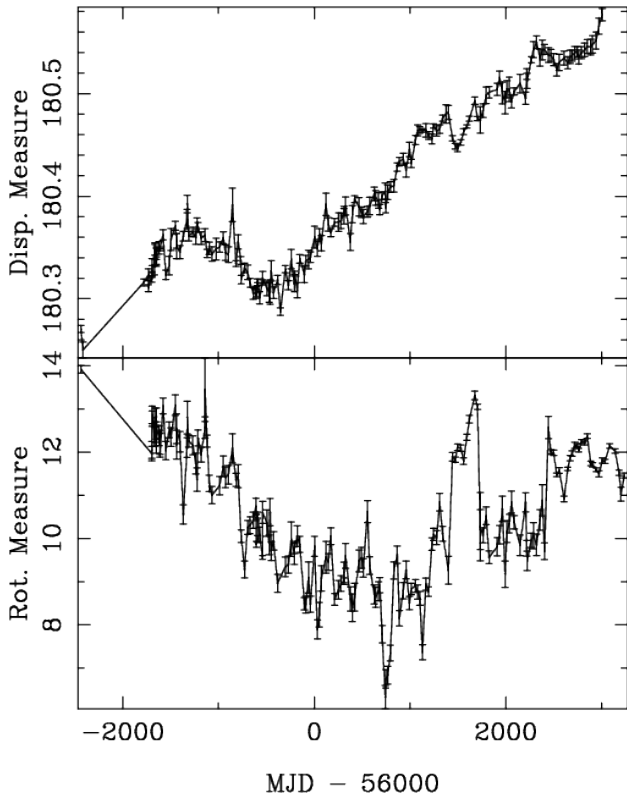


Figure 4. Dispersion Measure (top panel) and Rotation Measure (bottom panel) as a function of MJD for PSR J0908–4913.

5 VELOCITY VECTOR AND THE ORIENTATION OF THE ROTATION AXIS

There exists a remarkable correlation between the orientation of a pulsar’s rotation axis and its direction of proper motion. First found in radio pulsars by [Johnston et al. \(2005\)](#) based on a theoretical prediction by [Spruit & Phinney \(1998\)](#) and later confirmed via other radio ([Rankin 2007](#); [Noutsos et al. 2013](#)) and X-ray ([Helfand et al. 2001](#); [Ng & Romani 2004](#)) datasets, it appears to hold true for most, if not all, pulsars with an age less than about 10^5 yr. The geometry of PSR J0908–4913 is well established ([Kramer & Johnston 2008](#); [Johnston & Kramer 2019](#)). In brief, the angle between the rotation axis and the magnetic axis is 83.59° and that between the rotation axis and the line of sight is 91.03° . [Figure 3](#) shows the polarization profile of the pulsar at 8.5 GHz. At the location of the magnetic pole identified by [Johnston & Kramer \(2019\)](#), the position angle of the linear polarization is -38° . Remarkably, this is 88° away from the position angle of the proper motion. PSR J0908–4913 therefore emits in a mode orthogonal to the magnetic field lines and shows that the rotation axis and the proper motion vector are aligned (c.f. the Vela pulsar, [Johnston et al. 2005](#)).

6 DM AND RM VARIABILITY

Given the high proper motion of the pulsar, and its relatively close distance, we might expect to see variations in the pulsar’s dispersion measure and rotation measure (RM) over time. Indeed, in a comprehensive survey for DM variations carried out by [Petroff et al. \(2013\)](#), they found significant variations in the DM towards this pulsar. After

a gap of nearly 8 years, [Johnston et al. \(2021\)](#) showed that the DM variations had changed sign since the previous measurements.

The top panel in [Figure 4](#) shows the entire DM history (186 independent measurements) of this pulsar from MJD 53564 (2005 July) to MJD 59237 (2021 January). Apart from an initial gap at the beginning of the series, data have been taken with a monthly cadence since 2007 April. [Petroff et al. \(2013\)](#) used data between MJD 54220 and 56200 where the DM was largely decreasing. Since MJD 56000, the DM has been steadily increasing at a mean rate of $0.029 \text{ cm}^{-3} \text{ pcyr}^{-1}$. The RM towards the pulsar is rather low, yielding a mean magnetic field strength of $< 0.1 \mu\text{G}$ along the line of sight. This indicates the likely presence of reversals in the magnetic field direction in this direction. The RM history of the pulsar is given in the bottom panel of [Figure 4](#). Significant RM variations are seen, first a drop from 13 radm^{-2} to 9 radm^{-2} followed by a rise back to 12 radm^{-2} .

Both the DM and RM variations could be caused by the pulsar motion behind a filament from the SNR. Over the course of the 10 yr monitoring program, the pulsar has traversed a distance of some 7 mpc and in this time the DM has changed by $0.25 \text{ cm}^{-3} \text{ pc}$. This yields an electron density excess of some 35 cm^{-3} . With an RM change of 4 radm^{-2} over the same time period, this would imply a filament magnetic field of $20 \mu\text{G}$. These values are similar to those derived following RM and DM changes in the Vela pulsar ([Hamilton et al. 1985](#)) and in-line with what is expected for SNRs generally ([Reynolds et al. 2012](#)).

7 SUMMARY AND NEXT STEPS

More than 30 years after its original discovery, a complete picture of the remarkable pulsar PSR J0908–4913 is now beginning to emerge. Recent measurements of the pulsar’s proper motion show it to be a high velocity object, and the direction of its motion is exactly as predicted from the morphology of its associated bow-shock nebula ([Gaensler et al. 1998](#)). The orientation of the rotation axis is aligned with the proper motion vector once orthogonal-mode emission is taken into account. Examination of radio images of the Galactic plane in the vicinity of the pulsar reveal the presence of a putative SNR, G320.4–1.0. The pulsar appears to be on the edge of the SNR shell, with the proper motion vector pointing directly away from the SNR centre. If the association between G320.4–1.0 and pulsar is correct, then the pulsar can only be ~ 12 kyr old, significantly less than its characteristic age. Our preferred distance to the pulsar is 3 kpc, based on the lower limit from HI absorption and to ensure a velocity of less than 1000 kms^{-1} .

We plan to carry out very long baseline interferometry (VLBI) to obtain high angular resolution images of the PWN. This should allow us to determine the bow-shock stand-off radius in order to better understand the energetics of the system. X-ray observations in this direction are also warranted to supplement the previous data from [Kargaltsev et al. \(2012\)](#). Deep X-ray observations may well allow better constraints on the PWN and the relationship with the SNR, as has been done recently for PSR J1709–4429 and its putative parent remnant SNR G343.1–2.3 ([de Vries et al. 2021](#)).

Finally we note that [Yao et al. \(2021\)](#) have recently determined a full three dimensional picture of the motion of PSR J0538+2817 within its SNR via a combination of radio polarization and scintillation measurements. Such an approach should also be possible for PSR J0908–4913 through sensitive observations using the pulsar program on MeerKAT ([Johnston et al. 2020a](#)).

8 DATA AVAILABILITY

Pulsar data taken with the Parkes telescope are available via a public archive³. Data taken with the Compact Array are available via a public archive⁴. The Molonglo Galactic Plane Survey is available via FITS files⁵.

ACKNOWLEDGEMENTS

The Parkes telescope (*Murriyang*) and the Australia Telescope Compact Array are part of the Australia Telescope National Facility which is funded by the Commonwealth of Australia for operation as a National Facility managed by CSIRO. We acknowledge the Wiradjuri and Gomeri people as the traditional owners of the respective observatory sites. M.E.L. receives support from Australian Research Council Laureate Fellowship FL150100148, the Australian Government Research Training Program and CSIRO Space and Astronomy. We thank S. Mader for assistance with the 8 GHz observing, B. Posselt for useful comments and the referee for a timely review.

REFERENCES

- Abdo A. A., et al., 2013, *ApJS*, 208, 17
 Castelletti G., Dubner G., Golap K., Goss W. M., Velázquez P. F., Holdaway M., Rao A. P., 2003, *AJ*, 126, 2114
 Cordes J. M., Lazio T. J. W., 2002, arXiv e-prints, pp astro-ph/0207156
 D’Amico N., Manchester R. N., Durdin J. M., Stokes G. H., Stinebring D. R., Taylor J. H., Brissenden R. J. V., 1988, *MNRAS*, 234, 437
 Frail D. A., Scharringhausen B. R., 1997, *ApJ*, 480, 364
 Frail D. A., Giacani E. B., Goss W. M., Dubner G., 1996, *ApJ*, 464, L165
 Gaensler B. M., Frail D. A., 2000, *Nature*, 406, 158
 Gaensler B. M., Stappers B. W., Frail D. A., Johnston S., 1998, *ApJ*, 499, L69
 Green A. J., Cram L. E., Large M. I., Ye T., 1999, *ApJS*, 122, 207
 Hamilton P. A., Hall P. J., Costa M. E., 1985, *MNRAS*, 214, 5P
 Helfand D. J., Gotthelf E. V., Halpern J. P., 2001, *ApJ*, 556, 380
 Hobbs G., Lorimer D. R., Lyne A. G., Kramer M., 2005, *MNRAS*, 360, 974
 Johnston S., Karastergiou A., 2017, *MNRAS*, 467, 3493
 Johnston S., Kramer M., 2019, *MNRAS*, 490, 4565
 Johnston S., Nicastro L., Koribalski B., 1998, *MNRAS*, 297, 108
 Johnston S., Hobbs G., Vigeland S., Kramer M., Weisberg J. M., Lyne A. G., 2005, *MNRAS*, 364, 1397
 Johnston S., Karastergiou A., Willett K., 2006, *MNRAS*, 369, 1916
 Johnston S., et al., 2020a, *MNRAS*, 493, 3608
 Johnston S., Smith D. A., Karastergiou A., Kramer M., 2020b, *MNRAS*, 497, 1957
 Johnston S., et al., 2021, *MNRAS*, 502, 1253
 Jones L. R., Smith A., Angelini L., 1993, *MNRAS*, 265, 631
 Kargaltsev O., Durant M., Pavlov G. G., Garmire G., 2012, *ApJS*, 201, 37
 Koribalski B., Johnston S., Weisberg J. M., Wilson W., 1995, *ApJ*, 441, 756
 Kramer M., Johnston S., 2008, *MNRAS*, 390, 87
 Kramer M., Lyne A. G., Hobbs G., Löhmer O., Carr P., Jordan C., Wolszczan A., 2003, *ApJ*, 593, L31
 Lower M. E., et al., 2021, *MNRAS*. Submitted
 Manchester R. N., Kaspi V. M., Johnston S., Lyne A. G., D’Amico N., 1991, *MNRAS*, 253, 7P
 McKee C. F., Ostriker J. P., 1977, *ApJ*, 218, 148
 Murphy T., Mauch T., Green A., Hunstead R. W., Piestrzynska B., Kels A. P., Sztajer P., 2007, *MNRAS*, 382, 382
 Ng C. Y., Romani R. W., 2004, *ApJ*, 601, 479

- Ng C. Y., Romani R. W., Brisken W. F., Chatterjee S., Kramer M., 2007, *ApJ*, 654, 487
 Noutsos A., Schnitzeler D. H. F. M., Keane E. F., Kramer M., Johnston S., 2013, *MNRAS*, 430, 2281
 Parthasarathy A., et al., 2020, *MNRAS*, 494, 2012
 Petroff E., Keith M. J., Johnston S., van Straten W., Shannon R. M., 2013, *MNRAS*, 435, 1610
 Rankin J. M., 2007, *ApJ*, 664, 443
 Reardon D. J., et al., 2020, *ApJ*, 904, 104
 Reynolds S. P., Gaensler B. M., Bocchino F., 2012, *Space Sci. Rev.*, 166, 231
 Schinzel F. K., Kerr M., Rau U., Bhatnagar S., Frail D. A., 2019, *ApJ*, 876, L17
 Spruit H., Phinney E. S., 1998, *Nature*, 393, 139
 Stappers B. W., Gaensler B. M., Johnston S., 1999, *MNRAS*, 308, 609
 Taylor J. H., Cordes J. M., 1993, *ApJ*, 411, 674
 Yao J. M., Manchester R. N., Wang N., 2017, *ApJ*, 835, 29
 Yao J., et al., 2021, *Nature Astronomy*
 Zeiger B. R., Brisken W. F., Chatterjee S., Goss W. M., 2008, *ApJ*, 674, 271
 de Vries M., et al., 2021, *ApJ*, 908, 50

This paper has been typeset from a $\text{\TeX}/\text{\LaTeX}$ file prepared by the author.

³ <https://data.csiro.au/dap/>

⁴ <https://atoa.atnf.csiro.au/>

⁵ <http://www.astrop.physics.usyd.edu.au/MGPS/>